

Accepted Manuscript

Glacial-related morphology and sedimentary setting of a high-latitude lacustrine basin:
The Lago Chepelmut (Tierra del Fuego)

Jorge G. Lozano, Alejandro Tassone, Donaldo M. Bran, Emanuele Lodolo, Marco
Menichetti, María E. Cerredo, Federico Esteban, Juan P. Ormazabal, José Ísola,
Luca Baradello, Juan F. Vilas

PII: S0895-9811(18)30179-2

DOI: [10.1016/j.jsames.2018.06.020](https://doi.org/10.1016/j.jsames.2018.06.020)

Reference: SAMES 1960

To appear in: *Journal of South American Earth Sciences*

Received Date: 23 April 2018

Revised Date: 27 June 2018

Accepted Date: 27 June 2018

Please cite this article as: Lozano, J.G., Tassone, A., Bran, D.M., Lodolo, E., Menichetti, M., Cerredo, Mari.E., Esteban, F., Ormazabal, J.P., Ísola, José., Baradello, L., Vilas, J.F., Glacial-related morphology and sedimentary setting of a high-latitude lacustrine basin: The Lago Chepelmut (Tierra del Fuego), *Journal of South American Earth Sciences* (2018), doi: 10.1016/j.jsames.2018.06.020.

This is a PDF file of an unedited manuscript that has been accepted for publication. As a service to our customers we are providing this early version of the manuscript. The manuscript will undergo copyediting, typesetting, and review of the resulting proof before it is published in its final form. Please note that during the production process errors may be discovered which could affect the content, and all legal disclaimers that apply to the journal pertain.



Glacial-related morphology and sedimentary setting of a high-latitude lacustrine basin: The Lago Chepelmut (Tierra del Fuego)

Jorge G. Lozano^{1,2}, Alejandro Tassone^{1,2}, Donaldo M. Bran^{1,2}, Emanuele Lodolo³, Marco Menichetti⁴,
María E. Cerredo^{1,2}, Federico Esteban^{1,2}, Juan P. Ormazabal^{1,2}, José Ísola^{1,2}, Luca Baradello³, Juan F.
Vilas^{1,2}

(1) Universidad de Buenos Aires, Facultad de Ciencias Exactas y Naturales, Depto. De Ciencias Geológicas. Buenos Aires, Argentina

(2) CONICET-Universidad de Buenos Aires. Instituto de Geociencias Básicas, Aplicadas y Ambientales de Buenos Aires (IGeBA). Buenos Aires, Argentina

(3) Istituto Nazionale di Oceanografia e di Geofisica Sperimentale (OGS). Trieste, Italy

(4) Dipartimento di Scienze Pure ed Applicate, Università di Urbino, Italy

Abstract

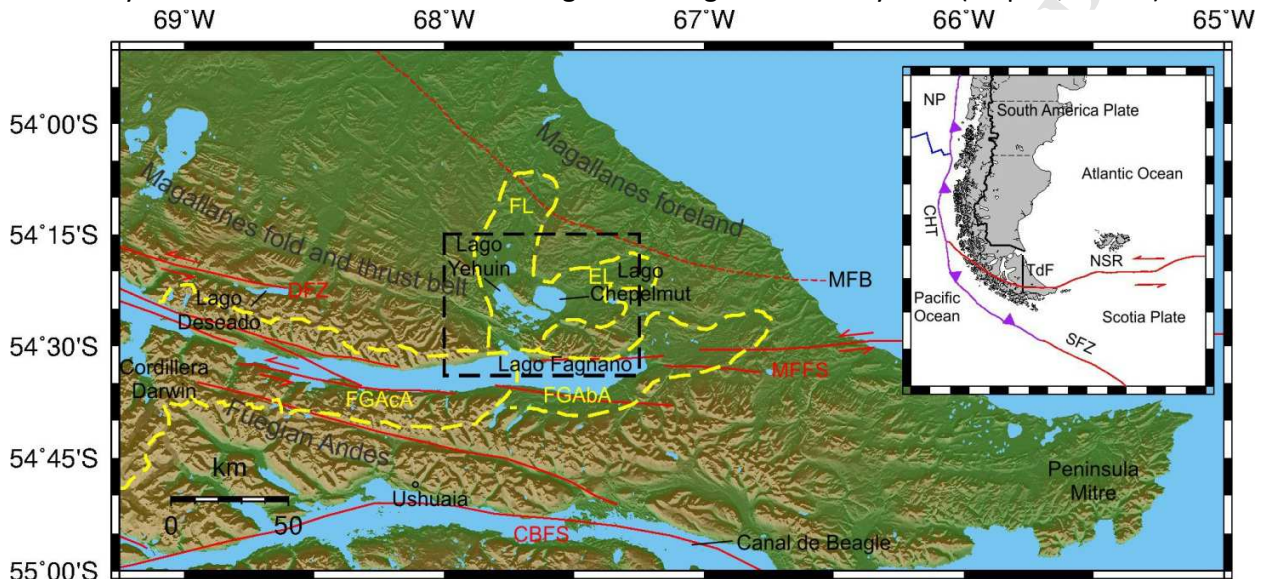
Lago Chepelmut is a relatively small lake in size, of ellipsoidal shape, located in the outer fold-and-thrust belt of the Fuegian Andes (southernmost South America). High-resolution single-channel seismic profiles, integrated with geological information in the surrounding area, have allowed to reconstruct for the first time a bathymetric map of the lake and the architecture, distribution and thickness of the sedimentary cover. Two main seismic units were identified in the seismic records: (i) a Lower Unit of glacial nature, likely associated to the Last Glacial Maximum (LGM), and irregularly distributed through the basin, and (ii) an Upper Unit of lacustrine origin which drapes the entire basin. Submerged moraine deposits within the lake were also found from seismic data, and correlated with moraine arcs widespread distributed in the surroundings of the basin. These morphologies represent the recessional deposits left by the Ewan glacier lobe, one of the easternmost fronts of the Tierra del Fuego glaciers during the LGM. The lacustrine sedimentary record shows that the lake level was not constant through the recent history of the lake. Moreover, data analyses has shown that there is also an important structural component that has conditioned the evolution of the basin, in addition to that linked to glacial activity.

Keywords: Tierra del Fuego, Lago Chepelmut, single-channel seismic profiles, sedimentary sequences, glacial morphology, Quaternary evolution

1. Introduction

Lago Chepelmut is located in the southernmost Andes, in Isla Grande de Tierra del Fuego (Figure 1), an area where superposed tectonic phases occurred since the Mid Cretaceous, in combination with

40 repeated glacial events, have significantly shaped the landscape (see Menichetti et al., 2008, and
 41 references therein). The basin lies just to the north (12 km) of Lago Fagnano, the largest freshwater
 42 lake in the entire island, interpreted as a pull-apart basin developed within the principal deformation
 43 zone of the Magallanes Fagnano Fault System, which marks the western segment of the South
 44 America-Scotia transform boundary (Lodolo et al., 2002, 2003; Esteban et al., 2012, 2014, among
 45 others). Several kilometers to the west of Lago Chepelmut, the Deseado Fault Zone appears as a
 46 subsidiary structure associated with the Magallanes-Fagnano Fault System (Klepeis, 1994b).



47
 48 Figure 1. Physiographic and structural provinces in Isla Grande de Tierra del Fuego. Magallanes fold
 49 and thrust belt corresponds to the external fold and thrust belt; Fuegoian Andes corresponds to
 50 the internal fold and thrust belt. The red dashed line is the thrust front of the Magallanes fold
 51 and thrust belt (MFB). Magallanes-Fagnano Fault System (MFFS), Canal de Beagle Fault System
 52 (CBFS) and Deseado Fault Zone (DFZ) are also indicated in red lines. FGAbA: Fagnano glacier
 53 ablation area; FGAcA: Fagnano glacier accumulation area; FL: Fuego ice lobe; EL: Ewan ice
 54 lobe. The inset box shows the current plate tectonic frame of the southern tip of South
 55 America and Scotia Sea. NP: Nazca Plate; CHT: Chile Trench; TdF: Tierra del Fuego; NSR: North
 56 Scotia Ridge. The black dashed box bounds the studied area.

57
 58 The Lago Chepelmut, which displays an ellipsoidal shape (average major and minor axis of 8
 59 and 5 km, respectively), is located in a low altitude zone (between 900 and 50 m.a.s.l.) within the
 60 “Corazón de la Isla” Provincial Reserve. The lake, along with the Lago Yehuín, are the two main
 61 freshwater lacustrine bodies within the reserve and in the Fuegoian steppe. Río In connects both basins
 62 and provides the water input from Lago Chepelmut to Lago Yehuín (Figure 2).

63 A series of geophysical surveys have been conducted in Tierra del Fuego region since 2001,
 64 primarily focusing in deciphering the tectonic evolution of the South America-Scotia plate during the
 65 Cenozoic (Esteban et al., 2011, 2014; Lippai et al., 2004; Lodolo et al., 2002, 2003, 2007; Menichetti et
 66 al., 2001, 2007a and b, 2008; Tassone et al., 2005, 2010, 2011; Waldmann et al., 2008, 2009, 2010a,

67 b). Several works, mainly of geophysical nature, have been devoted to other Fuegian lakes, i.e. Lago
68 Fagnano (Lippai et al., 2004; Zanolla et al., 2011; Waldmann et al., 2008, 2010, 2011; Esteban et al.,
69 2014), Lago Roca (Lodolo et al., 2010) and, more recently, Lago Yehuin (Lozano et al., 2018).

70 The main objective of this work is to reconstruct the genesis of Lago Chepelmut basin and
71 analyze the nature, depositional architecture and thickness of the sedimentary infill from the
72 interpretation of high-resolution seismic records acquired within the lake. This represents the first
73 geophysical survey performed in the lake. Almost 23 km of profiles were acquired and used to present
74 a new bathymetric map of the lake, to reconstruct the geometry and morphology of the cover, and
75 analyze the possible relationship between pre-existing structures and the recent sedimentary setting.

76 This study contributes to the knowledge of the lake evolution during the Quaternary and
77 analyzes its depositional history in an environment that was strongly affected by glacial activity,
78 within a complex geological setting presently dominated by strike-slip tectonics.

80 **2. Regional and geologic framework of Lago Chepelmut**

81 **2.1. The Fuegian Andes**

82 The regional geologic history of the Fuegian Andes is the product of a succession of contrasting
83 tectonic regimes. A widespread extensional regime in the Late Jurassic was established along the
84 southern Patagonian and Fuegian continental margin which resulted in the formation of the Rocas
85 Verdes marginal basin and the silicic volcanic deposition of Lemaire or Tobífera Formation (Dalziel et
86 al., 1974; Suárez and Pettigrew, 1976; Hanson and Wilson, 1991; Calderón et al., 2007). An extended
87 fault array consisting of N- to NW-oriented grabens and half-grabens and E- to NE-oriented transfer
88 faults were developed within this Jurassic stage (Ghiglione et al., 2013). Since the Late Jurassic to Early
89 Cretaceous, the stretching produced oceanic floor in the Rocas Verdes basin (Mukasa and Dalziel,
90 1996; Calderón et al., 2007), which was filled by Early Cretaceous marginal marine to arc-derived
91 sequences, such as the Yaghan, Beauvoir, Zapata, Erezcano and Hardy formations (Olivero and
92 Martinioni, 2001; Fildani and Hessler, 2005, Torres Carbonell et al., 2014). During the Late Cretaceous,
93 a compressive tectonic regime in the Pacific margin of the South America Plate (i.e., the Andean
94 Orogeny) led to the closure and inversion of the Rocas Verdes basin and to the development of the
95 fold and thrust belt (Dalziel et al., 1974; Bruhn, 1979; Nelson et al., 1980; Wilson, 1991; Klepeis,
96 1994a; Diraison et al., 2000; Kraemer, 2003; Menichetti et al., 2008; Klepeis et al., 2010; Torres
97 Carbonell et al., 2011, 2013).

98 During the Paleocene – Early Eocene, an extensional period characterized the area (Dalziel and
99 Brown, 1989; Galeazzi, 1998; Ghiglione et al., 2008, 2010), with the development of extensional
100 structures recognized near Canal de Beagle (Dalziel and Brown, 1989) and offshore in the Malvinas
101 Basin (Galeazzi, 1998; Baristead et al., 2013). Later, during the Late Eocene, the tectonic regime
102 changed to a further compressive period and the propagation of the fold and thrust belt (Ghiglione,
103 2016).

104 Finally, a strike-slip tectonic regime was established during the Cenozoic in the central and
105 southern area of the Tierra del Fuego, coeval with the formation of the Scotia Plate and its northern

106 boundary with the South America Plate, represented by the Magallanes-Fagnano fault system (Klepeis
107 and Austin, 1997; Diraison et al., 2000; Lodolo et al., 2002, 2003; Ghiglione and Ramos, 2005). Since
108 then, this transform boundary accommodates the relative movement between South America and
109 Scotia plates. The associated structures are mainly transtensional in nature, with the development of
110 pull-apart basins along the main wrench faults (Lodolo et al., 2003; Menichetti et al., 2008). The
111 Deseado Fault Zone (Figure 1) is one of the secondary structures associated with the plate boundary
112 and with the Magallanes-Fagnano Fault System. The Deseado Fault Zone is a linear structure about 50
113 km long with a left-lateral movement and associated extensional component which runs across Lago
114 Deseado, in the Chilean territory, outside the studied area (Klepeis, 1994b).

116 **2.2. Geology and morphology of the Lago Chepelmut area**

117 The main structural features of the Lago Chepelmut area are represented by NE-verging thrusts, with
118 a morphology characterized by elongated NW valleys (Figure 2; Buatois and Camacho, 1993). The
119 landscape surrounding the lake displays a smooth relief of elongated mounds, crossed by small and
120 mostly rectilinear valleys. These valleys run parallel to the mounds with an N direction and parallel to
121 the lake margin. The area, located in the central part of Isla Grande de Tierra del Fuego, exposes a
122 succession of Lower Cretaceous to Eocene units outcropping along WNW-oriented belts (Figure 2;
123 Malumián and Olivero, 2006; Olivero and Malumián, 2008; Martinioni et al., 2013). The Lower
124 Cretaceous Beauvoir Formation is found along the northern margin of Lago Fagnano; it is part of the
125 fill of the former Rocas Verdes marginal basin, and is composed of slates, mudstones and subordinated
126 sandstones of hemipelagic deep-marine environment. The Upper Cretaceous formations of Arroyo
127 Castorera, Río Rodríguez and Policarpo are mudstone-dominated, with an upward increase in coarse
128 sand material and represent the transition to the Late Cretaceous Austral foreland basin evolution.
129 This transition is interpreted as a turbiditic deposits that were progressively accumulated in front of
130 the rising Fuegian Andes (Martinioni et al., 2013). The exposures of Policarpo Formation in the vicinity
131 of Lago Chepelmut display a fairly constant WNW strike and are often affected by thrusting (Buatois
132 and Camacho, 1993, Torres Carbonell et al., 2013). The Paleocene Tres Amigos Formation (known as
133 Cerro Apen Beds in Martinioni et al., 2013) consists of conglomerates, sandstones and siltstones from
134 fan delta deposits. Leticia and Cerro Colorado formations, both from Eocene of La Despedida Group
135 (Martinioni et al., 2013), crops out in the northeast area, near the Lago Chepelmut. These formations
136 consist of grey to green sandstones of SW dip, intercalated with yellow mudstones and sandstones of
137 a coastal environment (Malumián and Olivero, 2006).

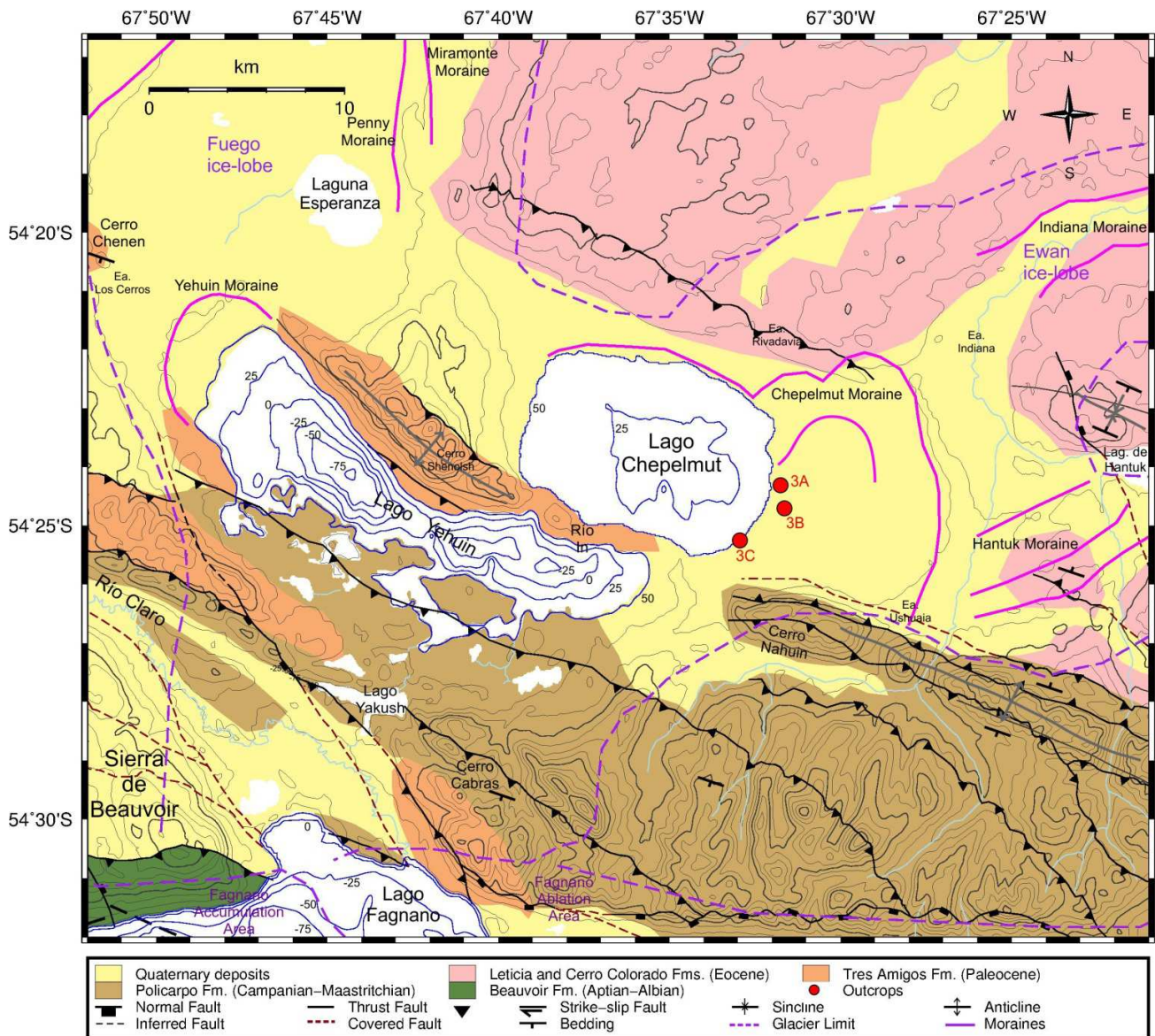


Figure 2. Geologic map of the Lago Chepelmut and its surroundings. Location is displayed in Figure 1. The bathymetry of the Lago Chepelmut (from this paper), Lago Yehuin and Lago Fagnano are also shown. Map adapted from Buatois and Camacho (1993), Menichetti et al. (2008), Martinioni et al. (2013), Torres Carbonell et al. (2013) and Esteban et al. (2014). Red dots show the position of some of the studied outcrops in the area, with the reference to the respective figure. The purple dashed lines enclose the area of the Fagnano palaeo-glacier, Fuego and Ewan glacier lobes after Coronato et al. (2009).

A significant proportion of the surrounding area of Lago Chepelmut is dominated by Quaternary deposits, mostly of glacial origin. During the Late Pleistocene, glaciers originating from the Cordillera Darwin ice sheet flowed to the east (Caldenius, 1932; Meglioli, 1992; Bujalesky et al., 1997). During the Last Glacial Maximum (LGM), ca. 25 ky B.P., multiple tributary glaciers flowed from the

151 northern and southern sides of the Fagnano glacier (Coronato et al., 2009; Rabassa et al., 2011) which
152 drained into the Atlantic Ocean through four main lobes (Figure 1). Among these, two ice-tongues
153 (i.e., Fuego and Ewan), flowed through the studied area (Figure 2), as evidenced by the presence of
154 frontal moraines along the valleys of Fuego and Ewan rivers (Coronato et al., 2008a, b). The
155 Chepelmut moraine (Figure 3A) is located at the eastern side of the lake, and it represents the most
156 proximal onland moraine of the Ewan valley. Its elevation is between 100 and 200 m.a.s.l. and is
157 distributed along the northern margin of Lago Chepelmut. An inner arc of the moraine with an
158 elevation between 70 and 100 m.a.s.l. is observed next to the eastern margin of the lake.

159 The Lago Chepelmut, together with Lago Yehuin and Lago Fagnano, were included in an older
160 moraine-dammed lake known as Paleolago Fueguino, which drained their waters to the Atlantic.
161 Progressively, this lake drained and decreased their water level, and left evidence in the sedimentary
162 deposits within the lakes (Del Valle et al., 2007). The most notable features are the fluvial terraces in
163 the Ewan river valley and the lake terraces along the eastern margin of Lago Chepelmut (Figure 3B).

164 Near the eastern margin of Lago Fagnano, the basal till that overlies the glacio-lacustrine and
165 glacio-fluvial deposits is composed by sedimentary breccia which includes boulder of siltstone,
166 sandstone and fossil peat. In other locations, laminated clayey-sandy silts overlie gravel beds, and
167 yellowish grey, fine sands with planar-parallel bedding are also recognized (Bujalesky et al., 1997). At
168 the eastern margin of the Lago Chepelmut, cross-bedded sands with some gravel layers compose the
169 post-glacial deposits (Figure 3C).

170



171

172

173

174

175

176

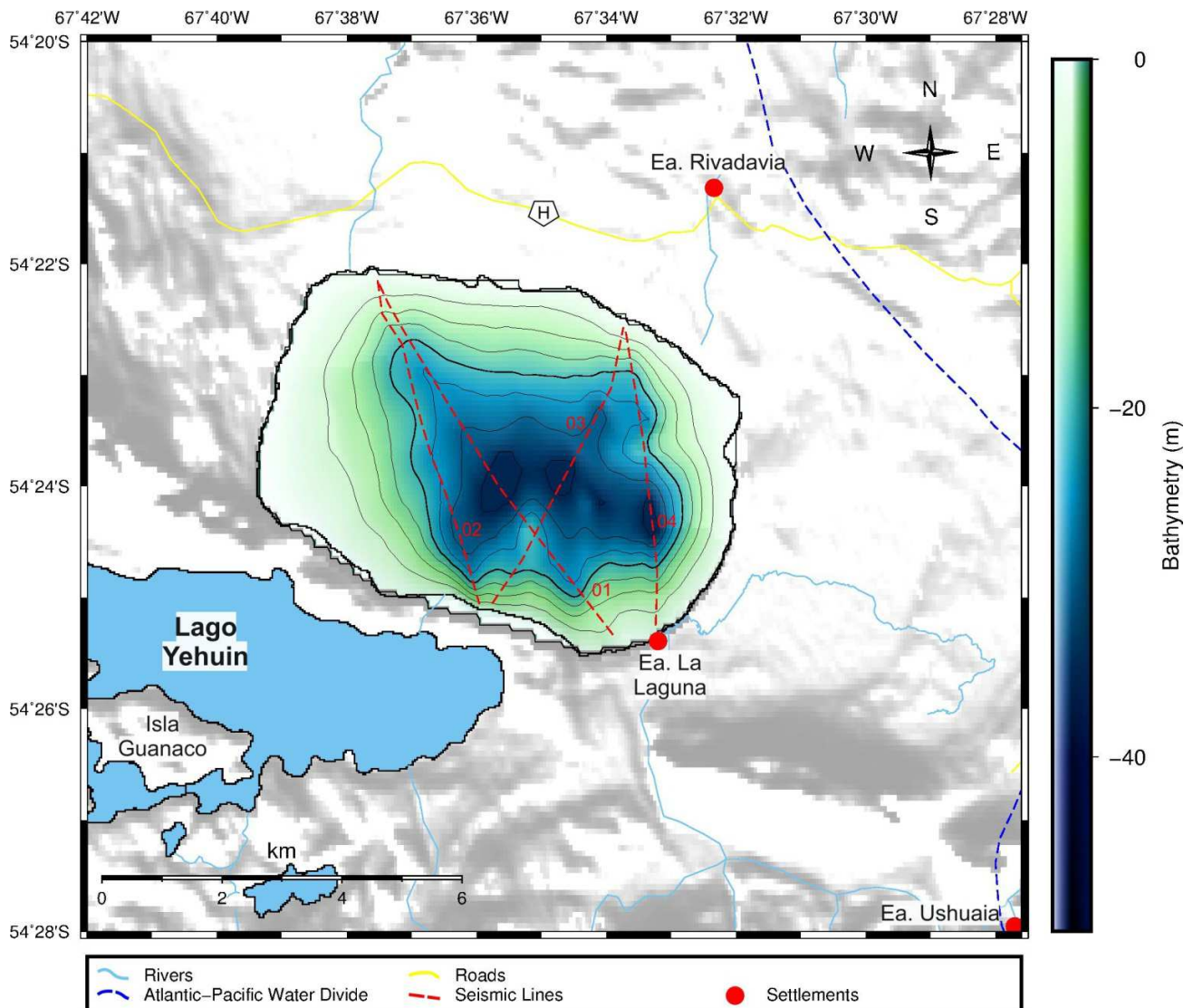
177

178

Figure 3. Landscape details and outcrops in the Lago Chepelmut area (location in Figure 2). A) An east-view of the inner arc of the Chepelmut moraine, pointed with an arrow. B) Lake terraces located at the eastern margin of the Lago Chepelmut. The terraces represent older stages of the lake shoreline. C) Deposits of a dissected lake terrace at a river meander with cross-bedded sands.

3. Data acquisition

179 In the period March-April 2014, four high-resolution, DGPS-navigated single-channel seismic profiles
180 were acquired in the Lago Chepelmut (Figure 4). The acquisition, performed on board a Zodiac boat,
181 was carried out with a Boomer as a seismic source and a 10-m-long streamer (see Donda et al., 2008,
182 Baradello and Carcione, 2008, Lodolo et al., 2012, for technical details of the H-R system used).
183 Sampling rate was 50 μ s, and the recording length 400 ms. Along-track horizontal resolution of 1 trace
184 every 1.0 m was achieved shooting at 0.5 s interval (at an average speed of 4 knots). Data were first
185 edited for noise traces, and a time-variant filtering and spike deconvolution were applied to improve
186 the signal/noise ratio. To obtain the final version of the profiles for interpretation, we applied on
187 traces the spherical divergence correction and an automatic gain (10 ms). The seismic profiles have
188 been uploaded, displayed and interpreted using the Kingdom Suite[®] software package (version 8.3).
189 To convert the two-way travel time of the high-resolution profiles to depth, we have assumed
190 different sound velocities based on the observable characteristics of each defined seismic unit and
191 according to the glacial deposits studied by Pugin et al. (1999). A water sound velocity of 1432 m/s
192 was used to produce the lake bathymetry, following Zanolla et al. (2011). Grids were created applying
193 a Kriging method. In order to remove incoherent data, minor editing was applied to these grids.
194 Considering that it has not been possible to create a regular grid of seismic lines to completely and
195 evenly cover the lake due to the often severe weather conditions, the construction of the bathymetric
196 map has required some interpolations. One of them was made assuming certain uniform bathymetry
197 between the beginning of each line and the shoreline, and smoothing significantly the automatic
198 contour produced by the algorithm from one line to the adjacent. For the thicknesses grids, data were
199 also interpolated between the four lines, assuming a virtual absence of sedimentary thickness in the
200 proximity of the lake margins. However, to verify the coherence between the thickness maps of the
201 two interpreted seismic units and the total sedimentary infill, a stacking of the grids was made to
202 check that no incoherent values exist between the stacked lower and upper units and the directly
203 calculated total sedimentary infill. Finally, the GMT software (Wessel and Smith, 1991) was used to
204 generate all the maps presented in this work.



205
 206 Figure 4. The Lago Chepelmut area with the main geographic references and settlements. The
 207 location of the acquired seismic lines is displayed in red dashed lines. The drainage net in this
 208 sector includes both Lago Yehuín and Lago Chepelmut. The blue dashed line is the
 209 Atlantic/Pacific water divide. In addition, the bathymetric map of the Lago Chepelmut is
 210 displayed, showing the deepest zone of the lake near the center of the basin. The lake
 211 shoreline is located at 52 m.a.s.l.; contour lines are every 5 meters.

212

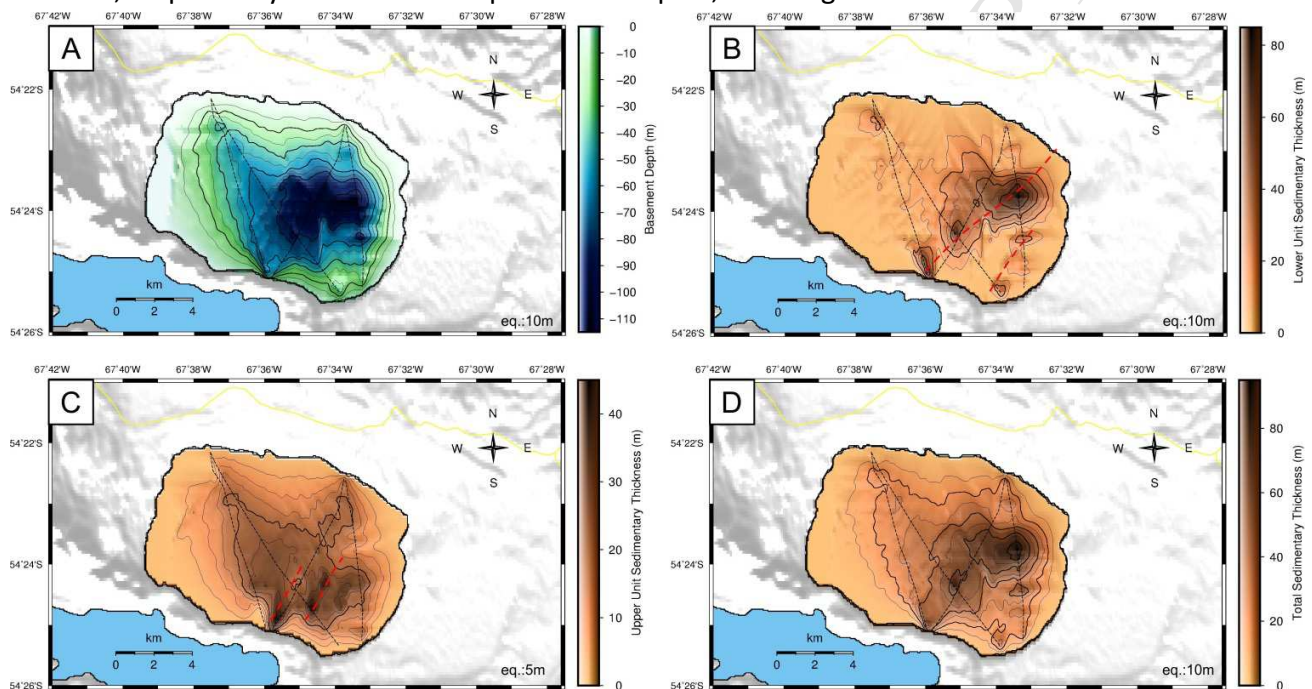
213 4. Seismic record of Lago Chepelmut

214 4.1. Bathymetry and acoustic basement

215 The high-resolution seismic lines provided the information to produce the bathymetric map of the
 216 Lago Chepelmut (Figure 4). This map shows a deepest zone of almost 40 m located near the center of
 217 the lake. The margin slopes are relatively smooth, mainly in the western part (0.7° in the western and
 218 1.7° in the eastern margin, respectively). The northern and southern margins are slightly steep (0.9°

219 and 1.4° , respectively). Some mound-shaped structures are located near the southern and eastern
 220 side at 15 to 20 m water depth, respectively.

221 The substratum of the Lago Chepelmut is represented by the acoustic basement, which is
 222 characterized by low-amplitude, discontinuous reflectors with no internal arrangement or particular
 223 reflector termination. Figure 5A shows the topography of the basement top. The depth increases
 224 progressively from the margins to the center of the lake, in concordance with the bathymetric map.
 225 The maximum depth reached is almost 110 m near the mid part of the seismic line 03. The western
 226 slope is gently sloping (1.4°), while the northern and southern slopes are steeper, with angles of 1.8°
 227 and 3.2° , respectively. The eastern slope is the steepest, with angles between 3.8° to 4.2° .



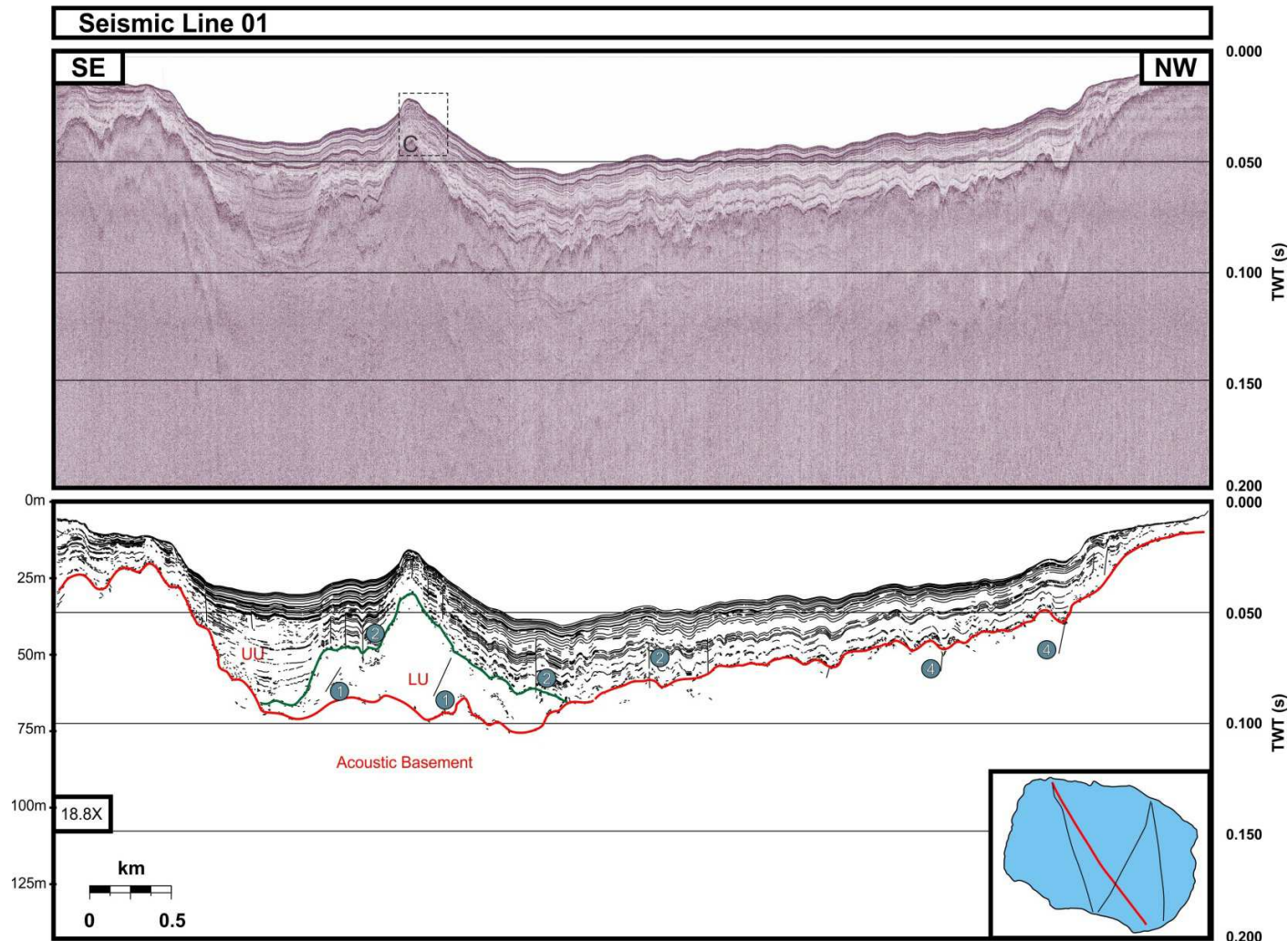
228
 229 Figure 5. A) Topographic map of the acoustic basement beneath the Lago Chepelmut, with a contour
 230 interval of 10 m. B) Map of the sedimentary thickness of the Lower Unit. The dashed red line
 231 indicates the NE orientation of the mounds. C) Sedimentary thickness of the Upper Unit. The
 232 dashed red line indicates the orientation of the deposits of the Upper Unit. D) Total
 233 sedimentary thickness.

234

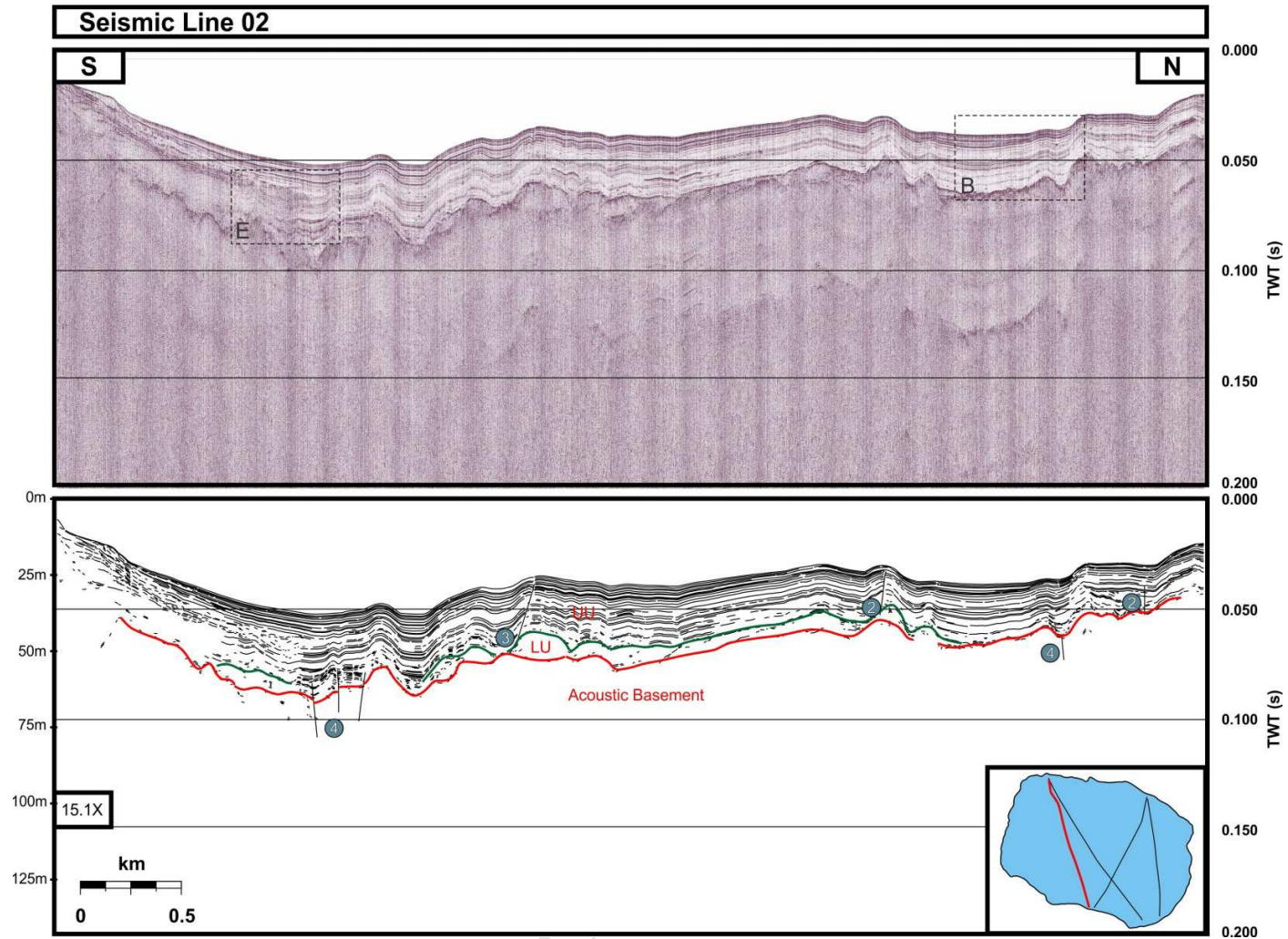
235 4.2. Seismic stratigraphy

236 The sedimentary infill of the Lago Chepelmut has been differentiated into two seismic units on the
 237 basis of geometric patterns and internal architecture of the seismic reflectors: The Lower Unit, which
 238 can be well recognized in the seismic lines 01 (Figure 6) and 04 (Figure 8) by their particular mound-
 239 like geometry; the Upper Unit, which covers the entire basin and smooth the topography (Figure 7).

240

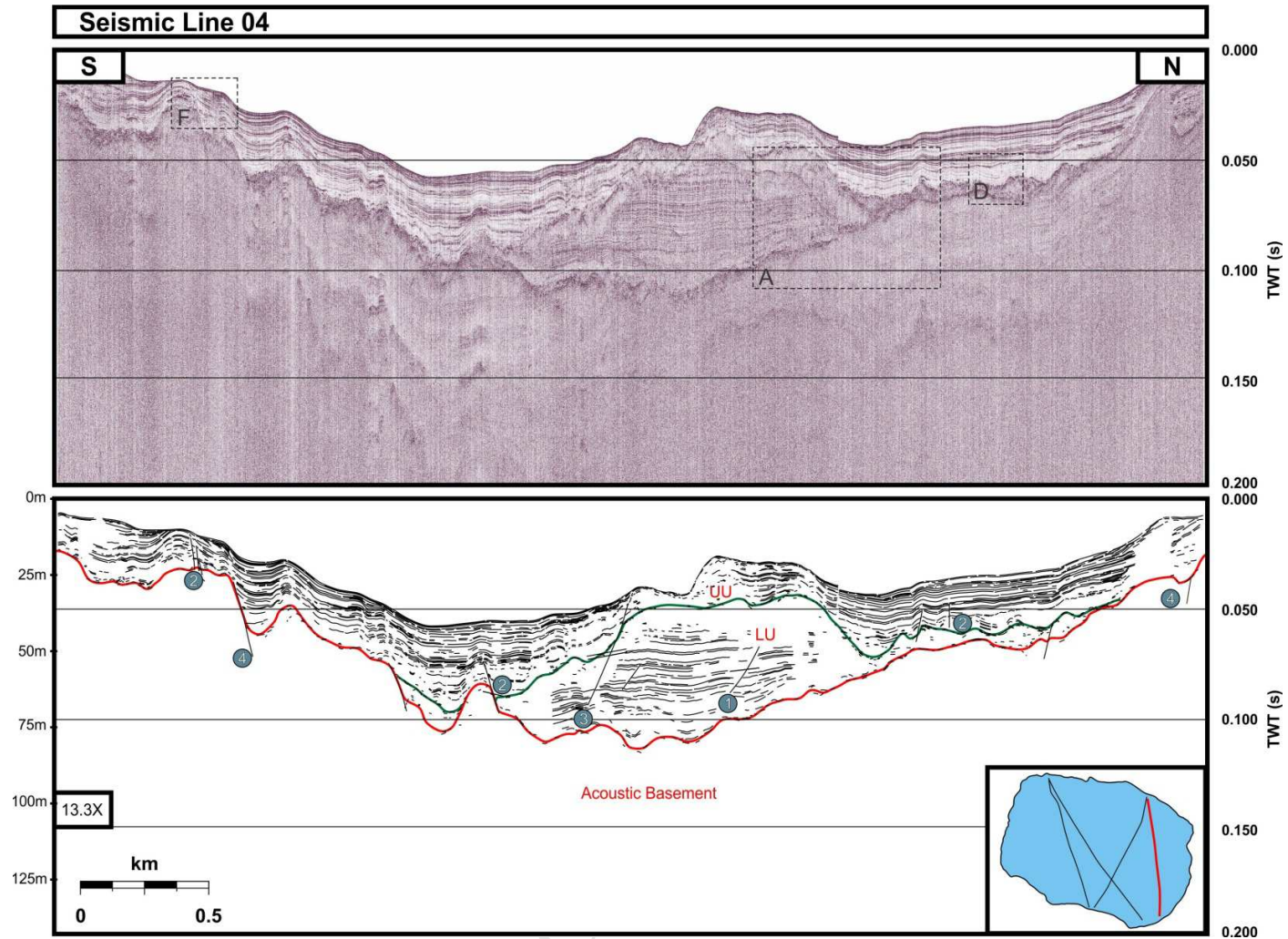


241
 242 Figure 6. Above, uninterpreted N-S high resolution single-channel seismic profile 01. Below, interpreted sketch with the reflector
 243 configuration and lineaments. Depth is given in two-way traveltime (TWT) and converted -only for this figure and as a qualitative
 244 measure - to sub-lake level depth (m) based on a P-wave velocity of 1432 m/s. The vertical exaggeration is shown in the lower
 245 left side of the interpreted section. The black lines are interpreted as normal faults. Numbers show the group of the faults
 246 according to the affected units; LU is the Lower Unit; UU is the Upper Unit. Details of the seismic sections are shown in the
 247 Figure 9.



248
 249
 250
 251

Figure 7. Above, un-interpreted N-S high resolution single-channel seismic profile 02. Below, interpreted sketch with the reflector configuration and lineaments. References same as Figure 6.



252

253

254

Figure 8. Above, un-interpreted N-S high resolution single-channel seismic profile 04. Below, interpreted sketch with the reflector configuration and lineaments. References same as Figure 6.

255

256 The Lower Unit (Figure 9A) rests over the acoustic basement and is chiefly developed in the
257 eastern half of the basin reaching a thickness of up to ~80 m in the central basin. For the time-depth
258 conversion, a sound velocity of 2600 m/s was assumed (see Pugin et al., 1999). Overall the Lower Unit
259 displays a mound-like geometry, grouped in three small mounds (Figure 5B). It is composed by seismic
260 reflectors which include low-amplitude, high to medium intensity, discontinuous with a parallel to
261 subparallel configuration, sometimes chaotic and with transparent intervals.

262 The Upper Unit (Figure 9B) comprises the sedimentary record between the lake bottom and
263 the top of the Lower Unit. For the time-depth conversion, a sound velocity of 1600 m/s was assumed
264 for this unit. It is mainly characterized by layered and continuous reflectors with a draped distribution
265 which fills the depressions of the underlying unit. The maximum thickness of almost 40 m is reached
266 near the southern margin; the center of the basin has an average of 40 m. The Upper Unit becomes
267 thinner towards the eastern and northern margins. In addition, there is a poorly defined NE trend for
268 the distribution of this unit in the southern margin (Figure 5C).

269 There are a few variations in the reflector geometries within this unit. The parallel intervals
270 sometimes appear to be truncated by erosive unconformities. In other cases, the reflectors become
271 chaotic with no internal arrangement, evidencing disturbed zones. The upper parts of the unit show
272 wedging reflectors to the margins.

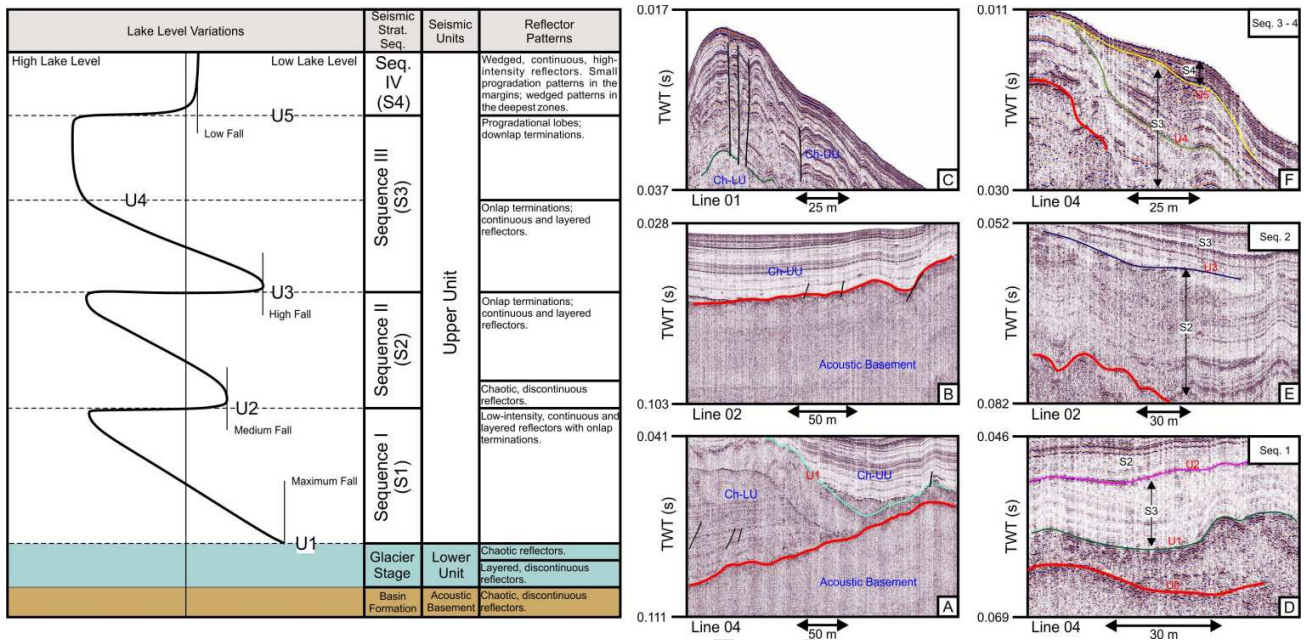
273 Both seismic units make up a total sedimentary package within the Lago Chepelmut basin of
274 almost 90 m of thickness in the deepest part of the basin (Figure 5D). The deposits appear to be
275 distributed along a NE direction.

276

277 4.3. Unconformities

278 Several unconformities were recognized in the seismic profiles. Some of them are recognized in the
279 whole basin while others are of limited extension, mostly restricted to basin margins. The identified
280 unconformities are six. From the base to the top, the first one is located at the top of the acoustic
281 basement, and is defined by a continuous and high amplitude reflector, U0 (Figure 9D) corresponding
282 to an erosive surface extended in the entire basin. Upwards, another unconformity, U1, of regional
283 extension within the Lago Chepelmut basin is defined by an erosive truncation of the underlying
284 reflectors and onlap configuration of the overlying seismic reflectors (Figure 9D). It separates the
285 Lower Unit from the Upper Unit. The other four unconformities are located within the Upper Unit,
286 affecting the parallel reflectors. The U2 unconformity is an erosive truncation restricted to Lago
287 Chepelmut margins which becomes a paraconformity in the central basin (Figure 9D). A clear erosive
288 truncation is found along the southern margin of Lago Chepelmut basin, U3, which separates folded
289 underlying reflectors from the downlap overlying reflectors (Figure 9E). A local angular unconformity,
290 U4, is identified by an acoustic fabric characterized by the overlying reflectors downlapping against
291 the underlying reflectors (Figure 9F). U4 is located only in the shallower zones of the northern and
292 southern margins. The uppermost unconformity, U5, is a slight angular unconformity located through

293 the entire basin. The overlying reflectors wedge through the deepest zones, while the underlying
 294 reflectors are strongly parallel (Figure 9F).



295
 296 Figure 9. Lake level curve including the correlation with the seismic units and the main reflector
 297 patterns between the unconformities. Except U4, the unconformities were assigned with a
 298 qualitative lake level fall based on the extent and depth reached by each erosional surface. The
 299 location of the inset is displayed in the Figures 6, 7 and 8; the continuous lines represent the
 300 discontinuities interpreted as normal faults; colored lines are the six recognized
 301 unconformities.

303 4.4. Interpretation of structure from seismic images

304 Several sub-vertical to oblique discontinuities were recognized in the seismic records (Figure 9C).
 305 These discontinuities of seismic reflectors show an average time shift of 0.002 TWT s (an offset of 1.5
 306 m) and affect mainly the sedimentary infill. The slip of the reflectors is downslip; therefore, they are
 307 interpreted as normal faults.

308 The faults can be divided in four groups based on the affected seismic unit. The first group (see
 309 faults in Figure 6) is composed by a few short normal faults that affect only the Lower Unit. The angles
 310 of the fault planes vary from 4° to 9°. The second group includes normal faults that are affecting only
 311 the Upper Unit. This group is composed by faults with an average dip of 15°, extended from the top of
 312 the Lower Unit to the upper part of the Upper Unit (Figure 7). A few faults are vertical to sub-vertical
 313 (Figure 9C). The third group is characterized by a few faults only found in the center of the lake basin
 314 (Figure 8), affecting the entire sedimentary package (Lower and Upper units). The angles of these
 315 faults are low, between 10° and 13°. The fourth group is composed by vertical to sub-vertical faults
 316 that are affecting the acoustic basement. Mainly found in the southern margin (Figure 6, 8) these

317 faults are associated with a stepped morphology of the substratum. In this group of faults, the time
318 shift reaches 0.007 TWT s (almost 5 m offset).

319

320 **5. Interpretation of the data**

321 **5.1. Seismic units**

322 *Lower Unit*

323 This seismic unit includes layered strata and continuous internal reflectors. These types of units have
324 been interpreted in other periglacial lakes (Eyles et al., 2000; Waldmann et al., 2008, 2010a, 2010b;
325 Pinson et al., 2013) as till deposits. The geometry of the Lower Unit (Figure 5B) suggests mound-like
326 morphology, which can be interpreted as a moraine deposit, based on the similarity with glacier
327 deposits studied, for example, in Bahía Inútil and Estrecho de Magallanes (Chile), or Oak Ridges
328 Moraine, in Canada (Pugin et al., 1999; Fernández et al., 2017). The distribution of the deposits in top
329 view shows a NE orientation (Figure 5B). The onland moraine arcs (i.e. Chepelmut, Indiana or Hantuk
330 moraines) along with this new submerged moraine ridge complete the recessional path of the Ewan
331 ice lobe along the Ewan river valley (Figure 2). Therefore, we interpret the mound shaped deposits of
332 this unit as part of the Ewan ice lobe terminal moraines.

333

334 *Upper Unit*

335 The Upper Unit is essentially composed by layered and continuous reflectors of varied reflectivity. The
336 well-defined geometry, continuity and extension of the reflectors suggest lacustrine sedimentation.
337 However, a detailed analysis of the geometries and their terminations, supported by a comparison
338 with other studies (i.e. Lyons et al., 2011; Scholz et al., 1998), indicates variations in the
339 sedimentation rate and local presence of erosion. A sequential stratigraphic analysis was made by the
340 observation of the geometric patterns of the reflectors.

341

342 **5.2. Seismic sequence stratigraphy of the Upper Unit**

343 The stratal architecture of the Lago Chepelmut as revealed from seismic data analysis reflects
344 changing rates between the accommodation space and the sedimentation rate of the basin. Following
345 the principles of seismic sequence stratigraphy (Vail et al., 1977; Vail 1987; van Wagoner et al., 1987;
346 Scholz, 2001), the deposits of the Upper Unit within the Chepelmut basin can be divided into four
347 seismic stratigraphic sequences. These sequences are defined and separated on the basis of erosional
348 surfaces and angular unconformities, interpreted to have been formed during major drops in the lake
349 level.

350 S1 (Figure 9D), the oldest sequence, begins with a lowstand marked after the deposits of the
351 seismic unit interpreted as glacier till (Lower Unit). The general retreat of the glacier lobe resulted in
352 an increase in the water input to the system. Then, a transgressive system tract due to the lake level
353 rise is represented by the first lacustrine deposits of the base of Upper Unit, with onlap terminations.
354 No high-stand system tract is recognized after the transgression as no progradational pattern is

355 observed in the reflectors. The upper boundary of the sequence is marked by an erosive truncation
356 (U2), and may represent a falling stage of the lake level.

357 S2 (Figure 9E) represents the lake change level after the first lake-level fall. Near the
358 lowermost part of this sequence, the Upper Unit is composed by chaotic reflectors with a lenticular
359 geometry, which may represent a small delta or fan sedimentation located in the southwestern and
360 northeastern basin margins. The presence of these deposits is the result of the sedimentation after
361 the erosive conditions which generated the boundary between sequence I and sequence II. Over the
362 fan sedimentation, the continuous, layered and medium to high reflectivity reflectors with onlap
363 terminations, are interpreted as a transgressive system tract marked by a lake level rise.

364 The sequence S3 (Figure 9F) is bounded at the base by another erosive truncation (U3). The
365 erosional relief of U3 is the most notable and accentuated in comparison with the other
366 unconformities. Therefore, it represent the highest lake level fall. The lower part of this sequence is
367 interpreted as a transgressive system tract, while the upper part represents a high-stand system tract
368 composed by wedged and downlap reflectors. The base of these reflectors, therefore, are interpreted
369 as a maximum flooding surface (U4), which marks the highest lake level during the lifetime of the
370 sedimentation of the S3.

371 The sequence S4 (Figure 9F), the youngest sequence of the Chepelmut basin, is bounded at the
372 base by an important erosive truncation (U5) which can be recognized at the northern and southern
373 margins of the lake. The continuous, layered, high reflectivity and, slight-wedged reflectors may be
374 interpreted as a lowstand system tract. The wedged reflectors and the progradational lobes on the
375 southern margin suggests that the lake level was low enough to give this type of depositional
376 structures, with a sediment bypass towards the deepest sectors of the basin.

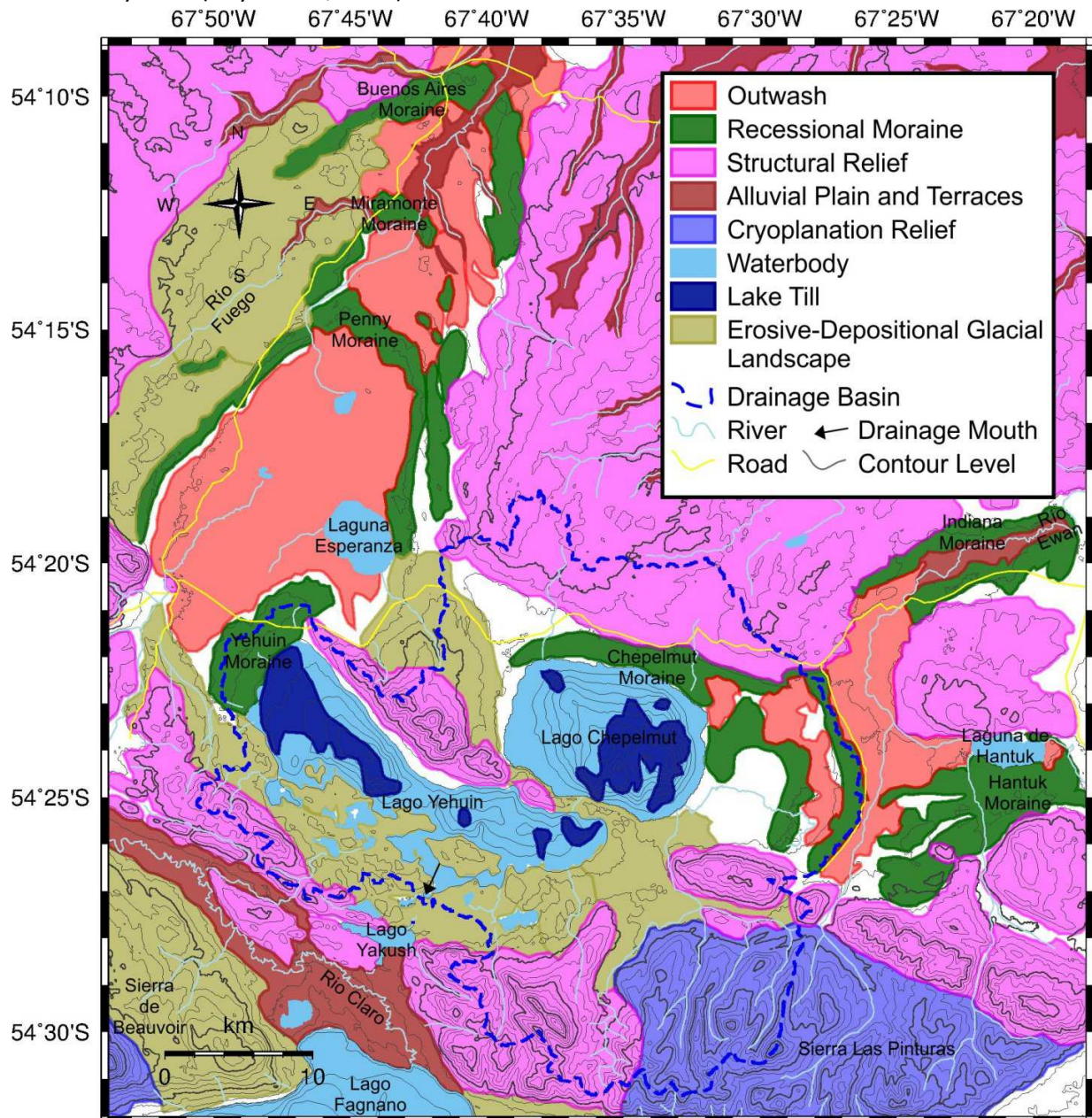
377 The described sequences reflect changing conditions in the lacustrine sedimentation within
378 the basin. The Figure 9 shows a schematic qualitative curve with the inferred lake level changes and a
379 correlation with the main events in the zone and with the previously defined seismic units.

380

381 **6. Discussion**

382 The glacial history of the central region of Tierra del Fuego has been documented both near the Lago
383 Fagnano (Bujaleski, 2011; Caldenius, 1932; Coronato et al., 2008a, b; 2009; Meglioli, 1992; Waldmann
384 et al., 2008; 2010 a, b) and near the Lago Yehuín and Chepelmut (Meglioli, 1992). Fuego and Ewan
385 glacier tongues, which were two diffluent ice lobes of the Fagnano glacier (Waldmann et al., 2010),
386 flowed northward and north-eastward, traversing both the Yehuín and Chepelmut basins (Lozano et
387 al., 2018). The exposed moraine deposits were mapped and dated in the Fuego and Ewan river
388 valleys. In the Fuego river valley, the Buenos Aires, Miramonte and Penny moraines can be correlated
389 with the stage B of the LGM (Coronato et al., 2008a), dated at 25.2 – 23.1 kyr B.P (McCulloch et al.,
390 2005). The Yehuín moraine is correlated with the stages C or D, of 21.7 – 20.3 kyr B.P. or older than
391 17.5 kyr B.P. In the Ewan river valley, the Indiana and Hantuk moraines are also correlated with the
392 stage B, while the Chepelmut moraine (Figure 3A) is correlated with the stages C or D (Coronato et al.,
393 2008b). Multiple advances/stillstands of the Fagnano glacier lobe were evidenced by moraine crests

394 preserved in the Fagnano lake basin (Waldmann et al., 2010). These oscillations probably had an
 395 effect on the retreat of the Ewan lobe. However, the final retreat of the glaciers from Tierra del
 396 Fuego's lowlands towards the Cordillera Darwin occurred during later stages of the Younger Dryas, at
 397 11 to 10 kyr B.P. (Boyd et al., 2008).



398
 399 Figure 10. Geomorphologic map of the Lago Yehuín and Lago Chepelmut area. The moraine arcs are
 400 displayed through the Fuego and Ewan river valleys. Additionally, the moraines within both
 401 lakes are also displayed. The blue dashed lines show the boundary of the drainage basin which
 402 is mainly controlled by the moraine arc at the western and eastern sides. The northern part is
 403 limited by a structural relief. The waters of the entire system output through the south,

404 toward Lago Fagnano. The glacial activity modeled the landscape and at present day, the
405 glacial deposits control the drainage.

406

407 A map with the geomorphology and the position of the moraines is presented in Figure 10. As
408 in the case of the Lago Chepelmut, submerged moraine ridges were interpreted in the sedimentary
409 record of the Lago Yehuín (Lozano et al., 2018). The Lago Yehuín shows thick deposits of glacial origin
410 located mainly in the western side, while in the eastern side are scarce. The differences in thickness
411 between the two sides of the Lago Yehuín are related with the two glacier lobes that move through
412 the area: the Fuego glacier lobe to the west and the Ewan glacier lobe to the east. In addition, the
413 difference in thickness could be due to the fact that the two glaciers (Ewan and Fuego) were different
414 in size and in sediment load, or maybe that the two glaciers melted in different times (Lozano et al.,
415 2018). The thickness of the glacial till of Lago Chepelmut is comparable with the glacial till of the
416 western side of Lago Yehuín.

417 The evidence of glacier dynamics and their deposits are mirrored in the sedimentary infill of
418 the Lago Chepelmut. The seismic analysis of the acquired profiles and the sedimentary architecture of
419 the lake fill suggests that the origin of the lake is due by the ice-carving of the Ewan glacier. However,
420 a primary control in the morphology could be due by the pre-existing structural setting of the area.
421 The Late Cretaceous compressive tectonics of the Magallanes fold and thrust belt developed a system
422 of W-NW thrust faults which is well represented in the relief and river valleys, mainly in the Sierra de
423 Beauvoir and Sierra Las Pinturas (Figure 2). It is well recognized that glaciers preferentially use already
424 formed structures as corridors for the ice flow. As an example, some studies show that there is a close
425 relationship between the structures related to wrench tectonics and the orientations of the fjords in
426 the southern Andes (Glasser and Ghiglione, 2009; Breuer et al., 2013). In other zones of Tierra del
427 Fuego, like the Lago Fagnano or the Canal de Beagle, a structural control is reported for the glacier
428 discharge patterns (Bujaleski, 2011; Lodolo et al., 2002, 2003). In the Ewan and Fuego river valleys,
429 existing structures related with the Jurassic transfer faults (Ghiglione et al., 2013) seem to be related
430 with the glacier path of the two glacier lobes. The strike-slip tectonics reactivated these older NE
431 Jurassic transfer faults and left their imprint in form of NE valleys like Fuego and Ewan river valleys
432 (Lozano et al., 2018). Finally, the glacier activity modeled the relief and later deposited the moraine
433 arc, locally changing the drainage net. The geomorphological map shows that there is a quite close
434 relationship between structural lineaments and the general trend of the rivers and valleys. A sub-
435 parallel to sub-dendritic drainage pattern is recognized in the area. The drainage basin observed in
436 Figure 10 shows that there is a main control from the glacier forms with the boundaries located in the
437 western and eastern areas of the lake. These depositional forms separate Ewan and Fuego river
438 valleys from the Lago Yehuín and Chepelmut.

439 The sedimentary patterns in lakes are controlled by allogenic factors such as tectonics and
440 climate through interactions of four main variables: sediment supply, water supply, basin-sill height
441 (spill point), and basin-floor depth (Bohacs et al., 2000; 2003). Erosional surfaces are best developed
442 on areas where relatively slow rates of subsidence limit accommodation space (Scholz et al., 1998).

443 The lake level curve (Figure 9) shows a progressive increase in the lake water level, which can be
444 inferred as the result of the enormous water input due to the melting of ice lobes and permafrost
445 during the climate warming after the LGM (Del Valle et al., 2007). The record of the changing lake
446 level is also evident from lake terraces located in the eastern margin of the Lago Chepelmut (Figure
447 3B). The decrement of the lake level, which left an evidence of three erosive unconformities (U2, U3
448 and U5) within the lacustrine deposits (Upper Unit) can be correlated with the three terraces levels
449 recognized along the Fuego river valley (Coronato et al., 2008a) and the three to four terraces levels
450 in the Ewan river valley (Coronato et al., 2008b). However, at present day, the Lago Chepelmut is
451 disconnected from the valley due to the low lake level (Figure 10). The youngest sequence IV,
452 therefore, represents a stage where the hydrology was characterized by drainage to the south,
453 through the Lago Fagnano. The change in the hydrology of the Lago Chepelmut from the Atlantic
454 water drainage to a drainage to Seno Almirantazgo (Estrecho de Magallanes, Chile) was established
455 7.8 kyr B.P., when the Paleolago Fueguino – a water body which includes the present day Lago
456 Fagano, Yehuín and Chepelmut – decreased their water level after the LGM. This decrease could be
457 associated to a seismic event in the area, which caused the broke of the moraine barriers of the lakes
458 and led to a loss of the water of the system (Del Valle et al., 2007). The unconformity U5 can be
459 correlated with this event and may be assigned an age of 7.8 kyr B.P.

460 The several faults recognized within the seismic sections, in particular, groups 1 to 3, are
461 characterized by low angles of 5° to almost 20° with a low offset. This deformation within the
462 sedimentary record can be treated as a result of a gravity collapse, given its low angle, low offset and
463 their presence confined only within the sedimentary package. However, it cannot be excluded that
464 these may have been generated by earthquakes. Seismological data of the Tierra del Fuego show a
465 great variety of seismic events that comprise earthquakes of low to medium magnitude, with the
466 majority of the events between 2 and 4 Mm, with 50% of them located in the uppermost 10 km. In
467 addition, seismicity shows that the zone is active at the present day (Buffoni et al., 2009; Sabbione et
468 al., 2007, 2016) and recent GPS studies conducted along the Magallanes-Fagnano Fault System
469 indicate that the principal strain components define two deformation styles: a zone with predominant
470 shortening of the crust to the west, and significant stretching to the east (Mendoza et al., 2011). NW-
471 SE extensional components and a subordinate contraction component with a SW-NE trend have been
472 reported for the Lago Yehuín area (Mendoza et al., 2011, 2015). Therefore, the Yehuín and Chepelmut
473 basins are located within an area dominated by transtensional, left-lateral deformation.

474 The fault group 4, characterized by vertical to sub-vertical normal faults which affect the
475 basement of the lake, could have a tectonic origin, so we cannot exclude *a priori* the occurrence of
476 tectonic factors which partly influenced the genesis and evolution of the Lago Chepelmut. A fault zone
477 analogous to the Deseado Fault Zone but located between Lago Yehuín and Chepelmut (Lozano et al.,
478 2018) could be the responsible of the normal faulting of the basement and the trigger for the gravity
479 collapse of the lacustrine sediments.

480

481 7. Conclusions

- 482 • Analysis and interpretation of single-channel seismic records, coupled with information
483 derived from outcrops, have allowed to produce for the first time a bathymetric map of the
484 Lago Chepelmut and analyze the sedimentary architecture of the depositional cover.
- 485 • The Lago Chepelmut, a small basin located in the central part of Tierra del Fuego Island, is
486 filled with sediments grouped into two units: a Lower Unit, consisting of glacial deposits, is
487 found in the deepest part of the lake, near the eastern margin. These till deposits were
488 correlated with onland moraine ridges to reconstruct the recessional path of the Ewan ice
489 lobe. The Upper Unit, interpreted of lacustrine origin, drapes the entire basin and represents
490 the sedimentation which occurred after the glacier retreat.
- 491 • After the moraine deposition in the Lago Chepelmut basin, the lacustrine stage was marked by
492 variations in the lake water level. At least three lake level falls were recognized from the
493 analysis of the sedimentary infill. However, the exact magnitude and the age constraints of
494 these variations remain difficult to determine.
- 495 • Data suggest that the origin of Lago Chepelmut basin is mostly due to ice-carving by glacier
496 lobes dynamics. However, the presence of a few vertical to sub-vertical faults affecting both
497 the basement of the Lago Chepelmut and part of the sedimentary cover testify that tectonic
498 activity has contributed to shape the lake.
- 499 • There is a tight correspondence between structural lineaments and ice flow paths of the Ewan
500 and Fuego glacial lobes. These structural-controlled corridors of ice discharge were later
501 reshaped by glacier activity.
- 502 • Several low-angle normal faults occur in the sedimentary infill of the Chepelmut basin which
503 can be related to gravity collapses. The Lago Chepelmut zone is located in a seismically active
504 area, where a complex array of left-lateral, strike-slip lineaments is developed. A fault zone
505 analogous to the Deseado Fault Zone, located between Lago Yehuin and Chepelmut, could be
506 the responsible of the normal faulting of the basement and possibly the trigger for the gravity
507 collapse of the sediments.

510 **Acknowledgments**

511 We acknowledge those people who contributed with field work in Tierra del Fuego: J.L. Hormaechea,
512 G. Connon, L. Barbero and C. Ferrer (EARG) for their support during data acquisition in the field, M.
513 Grossi (OGS) for seismic acquisition. Funds for this study were partly provided by the Italian Ministero
514 degli Affari Esteri (MAE) and the MiNCyT “La Agencia” PICT 2013-2236 projects and from CONICET PIP
515 Nro. 112201101 00618, Argentina. We are grateful for the constructive reviews made by the Editor, V.
516 Ramos, M. Ghiglione, and other three anonymous reviewers that greatly improved the original
517 manuscript.

518

519 **References**

- 520 Baradello, L., Carcione, J.M., 2008. Optimal seismic-data acquisition in very shallow waters: Surveys in
521 the Venice lagoon. *Geophysics*, 73 (6), 59-63.
- 522 Baristeas, N., Anka, Z., di Primio, R., Rodriguez, J.F., Marchal, D., Dominguez, F., 2013. New insights
523 into the tectono-stratigraphic evolution of the Malvinas Basin, offshore of the southernmost
524 Argentinean continental margin. *Tectonophysics*, 604, 280-295.
- 525 Bohacs, K.M., Carroll, A. R., Neal, J.E., Mankiewicz, P.J., 2000. Lake-basin type, source potential, and
526 hydrocarbon character: an integrated-sequence-stratigraphic-geochemical framework. In:
527 Gierlowski-Kordesch, E.H., Kelts, K.R. (Eds.), *Lake basins through space and time: AAPG*
528 *Studies in Geology*, 46, 3-34
- 529 Bohacs, K.M., Carroll, A.R., Neal, J.E., 2003. Lessons from large lake systems – Thresholds,
530 nonlinearity, and strange attractors. *Geological Society of America, Special Paper 370*, 75-90.
- 531 Boyd, B.L., Anderson, J.B., Wellner, J.S., Fernández, R.A., 2008. The sedimentary record of glacial
532 retreat, Marinelli fjord, Patagonia: regional correlations and climate Ties. *Marine Geology*, 255
533 (3-4), 165-178.
- 534 Breuer, S., Kilian, R., Schörner, D., Weinrebe, W., Behrmann, J., Baeza, O., 2013. Glacial and tectonic
535 control on fjord morphology and sediment deposition in the Magellan region (53° S), Chile.
536 *Marine Geology*, 346, 31-46.
- 537 Bruhn, R.L., 1979. Rock structures formed during back-arc basin deformation in the Andes of Tierra
538 del Fuego. *Geological Society of America Bulletin*, 90 (11), 998-1012.
- 539 Buatois, L.A., Camacho, H.H., 1993. Geología del sector nororiental del Lago Fagnano, Isla Grande de
540 Tierra del Fuego. *Revista de la Asociación Argentina*, 48 (2), 109-124.
- 541 Bujalesky, G.G., 2011. The flood of the Beagle Valley (11,000 yr BP), Tierra del Fuego. *Anales Instituto*
542 *Patagonia (Chile)*, 39, 5-21.
- 543 Bujalesky, G.G., Heusser, C.J., Coronato, A.M., Roig, C.E., Rabassa, J.O., 1997. Pleistocene
544 glaciolacustrine sedimentation at Lago Fagnano, Andes of Tierra del Fuego, Southernmost
545 South America. *Quaternary Science Reviews*, 16 (7), 767-778.
- 546 Buffoni, C., Sabbione, N.C., Connon, G., Ormaechea, J.L., 2009. Localización de hipocentros y
547 determinación de su magnitud en Tierra del Fuego y zonas aledañas. *Geoacta*, 34 (2), 75-86.
- 548 Caldenius, C.R.C., 1932. Las glaciaciones cuaternarias en la Patagonia y Tierra del Fuego: una
549 investigación regional, estratigráfica y geocronológica, una comparación con la escala
550 geocronológica sueca. *Dirección General de Minas y Geología*.
- 551 Calderón, M., Fildani, A., Herve, F., Fanning, C. M., Weislogel, A., Cordani, U., 2007. Late Jurassic
552 bimodal magmatism in the northern sea-floor remnant of the Rocas Verdes basin, southern
553 Patagonian Andes. *Journal of the Geological Society*, 164 (5), 1011-1022.
- 554 Coronato, A., Ponce, F., Sepälä, M., Rabassa, J., 2008a. Englazamiento del valle del rio Fuego durante
555 el Pleistoceno tardío, Tierra del Fuego, Argentina. *XVII Congreso Geológico Argentino, San*
556 *Salvador de Jujuy, Argentina*.

- 557 Coronato, A., Ponce, F., Rabassa, J., Sepälä, M., 2008b. Evidencias morfológicas del englazamiento del
558 valle del río Ewan, Tierra del Fuego, Argentina. XVII Congreso Geológico Argentino, San
559 Salvador de Jujuy, Argentina.
- 560 Coronato, A., Seppälä, M., Ponce, J.F., Rabassa, J., 2009. Glacial geomorphology of the Pleistocene
561 Lake Fagnano ice lobe, Tierra del Fuego, southern South America. *Geomorphology*, 112 (1-2),
562 67-81.
- 563 Dalziel, I.W.D., Brown, R.L., 1989. Tectonic denudation of the Darwin metamorphic core complex in
564 the Andes of Tierra del Fuego, southernmost Chile: Implications for Cordilleran orogenesis.
565 *Geology*, 17, 699-703.
- 566 Dalziel, I.W.D., de Witt, M.J., Palmer, K.F., 1974. Fossil marginal basin in the southern Andes. *Nature*,
567 250, 291-294.
- 568 Del Valle, R.A., Tatur, A., Rinaldi, C.A., 2007. Cambios en lagos y circulación fluvial vinculados al
569 calentamiento climático del Pleistoceno Tardío-Holoceno Temprano en Patagonia e Isla 25 de
570 Mayo, Islas Shetland del Sur, Antártida. *Revista de la Asociación Geológica Argentina*, 62 (4),
571 618-626.
- 572 Diraison, M., Cobbold, P.R., Gapais, D., Rossello, E.A., Le Corre, C. 2000. Cenozoic crustal thickening,
573 wrenching and rifting in the foothills of the southernmost Andes. *Tectonophysics*, 316 (1), 91-
574 119.
- 575 Donda, F., Brancolini, G., Tosi, L., Kovacevic, V., Baradello, L., Gacic, M., Rizzetto, F., 2008. The ebb-
576 tidal delta of the Venice Lagoon, Italy. *The Holocene*, 18 (2), 267-278.
- 577 Esteban, F.D., Tassone, A., Menichetti, M., Rapalini, A.E., Remesal, M.B., Cerrredo, M.E., Lippai, H.,
578 Vilas, J.F., 2011. Magnetic fabric and microstructures across the Andes of Tierra del Fuego,
579 Argentina. *Andean Geology*, 38 (1), 64-81.
- 580 Esteban, F.D., Tassone, A., Lodolo, E., Menichetti, M., 2012. The South America-Scotia plate boundary
581 from 67° W to 56° W (Southernmost Atlantic ocean). *Rendiconti Online Società Geologica
582 Italiana*, 22, 76-79.
- 583 Esteban, F.D., Tassone, A., Lodolo, E., Menichetti, M., Lippai, H., Waldmann, N., Darbo, A., Baradello,
584 L., Vilas, J.F., 2014. Basement geometry and sediment thickness of Lago Fagnano (Tierra del
585 Fuego). *Andean Geology*, 41 (2), 293-313.
- 586 Eyles, N., Boyce, J.I., Halfman, J.D., Koseoglu, B., 2000. Seismic stratigraphy of Waterton Lake, a
587 sediment-starved glaciated basin in the Rocky Mountains of Alberta, Canada and Montana,
588 USA. *Sedimentary Geology*, 130 (3), 283-311.
- 589 Fernández, R., Gulick, S., Rodrigo, C., Domack, E., Leventer, A., 2017. Seismic stratigraphy and glacial
590 cycles in the inland passages of the Magallanes Region of Chile, southernmost South America.
591 *Marine Geology*, 386, 19-31.
- 592 Fildani, A., Hessler, A.M., 2005. Stratigraphic record across a retroarc basin inversion: Rocas Verdes-
593 Magallanes Basin, Patagonian Andes, Chile. *Geological Society of America Bulletin*, 117 (11-
594 12), 1596-1614.

- 595 Galeazzi, J.S., 1998. Structural and stratigraphic evolution of the western Malvinas Basin, Argentina.
596 AAPG Bulletin, 82 (4), 596-636.
- 597 Ghiglione, M.C. Ramos, V.A., 2005. Progression of deformation and sedimentation in the
598 southernmost Andes. *Tectonophysics*, 405, 25-46.
- 599 Ghiglione, M.C., 2016. Orogenic growth of the Fuegian Andes (52-56°) and their relation to tectonics
600 of the Scotia Arc. In: Folguera, A., Naipauer, M., Sagripanty, L., Ghiglione, M.C., Orts, D.,
601 Giambiagi, L.B. (Eds.), *Growth of the Fuegian Andes*. Springer Earth System Sciences, 241-267.
- 602 Ghiglione, M. C., Navarrete-Rodríguez, A.T., González-Guillot, M., Bujalesky, G., 2013. The opening of
603 the Magellan Strait and its geodynamic implications. *Terra Nova*, 25 (1), 13-20.
- 604 Ghiglione, M.C., Quinteros, J., Yagupsky, D., Bonillo-Martínez, P., Hlebszevtich, J., Ramos, V.A.,
605 Vergani, G., Figueroa, D., Quesada, S., Zapata, T., 2010. Structure and tectonic history of the
606 foreland basins of southernmost South America. *Journal of South American Earth Sciences*,
607 29, 262-277.
- 608 Ghiglione, M. C., Yagupsky, D., Ghidella, M., Ramos, V.A., 2008. Continental stretching preceding the
609 opening of the Drake Passage: Evidence from Tierra del Fuego. *Geology*, 36 (8), 643-646.
- 610 Glasser N, Ghiglione, M.C., 2009. Structural, tectonic and glaciological controls on the evolution of
611 fjord landscapes. *Geomorphology*, 105, 291-302
- 612 Hanson, R.E., Wilson, T.J., 1991. Submarine rhyolitic volcanism in a Jurassic proto-marginal basin;
613 southern Andes, Chile and Argentina. *Geological Society of America Special Papers*, 265, 13-
614 28.
- 615 Klepeis, K.A., 1994a. A relationship between uplift of the metamorphic core of the southernmost
616 Andes and shortening in the Magallanes foreland fold and thrust belt, Tierra del Fuego.
617 *Tectonics*, 13, 882-904.
- 618 Klepeis, K.A., 1994b. The Magallanes and Deseado fault zones: major segments of the South
619 American-Scotia transform plate boundary in southernmost South America, Tierra del Fuego.
620 *Journal of Geophysical Research*, 99, 22001-22014.
- 621 Klepeis, K.A., Austin, J.A., 1997. Contrasting styles of superposed deformation in the southernmost
622 Andes. *Tectonics*, 16 (5), 755-776.
- 623 Klepeis, K., Betka, P., Clarke, G., Fanning, M., Hervé, F., Rojas, L., Mpodozis, C., Thomson, S., 2010.
624 Continental underthrusting and obduction during the Cretaceous closure of the Rocas Verdes
625 rift basin, Cordillera Darwin, Patagonian Andes. *Tectonics*, 29 (3).
- 626 Kraemer, P.E., 2003. Orogenic shortening and the origin of the Patagonian orocline (56°lat S). *Journal*
627 *of South America Earth Sciences*, 15, 731-748.
- 628 Lippai, H., Lodolo, E., Tassone, A., Hormaechea, J.L., Menichetti, M., Vilas, J.F., TESAC Party., 2004.
629 Morpho-structure of Lago Fagnano (Tierra del Fuego) and adjacent areas. *Bollettino di*
630 *Geofisica Teorica ed Applicata*, 45 (2), 142-144.
- 631 Lodolo, E., Menichetti, M., Tassone, A., Geletti, R., Sterzai P., Lippai, H. and Hormaechea, J.L., 2002.
632 Researchers target a continental transform fault in Tierra del Fuego. *EOS Transactions, AGU*,
633 83 (1), 1+5-6.

- 634 Lodolo, E., Menichetti, M., Bartole, R., Ben-Avraham, Z., Tassone, A., Lippai, H., 2003. Magallanes-
635 Fagnano continental transform fault (Tierra del Fuego, southernmost South America).
636 *Tectonics*, 22 (6).
- 637 Lodolo, E., Lippai, H., Tassone, A., Zanolla, C., Menichetti, M., Hormaechea, J.L., 2007. Gravity map of
638 the Isla Grande de Tierra del Fuego, and morphology of Lago Fagnano. *Geologica Acta*, 4, 307-
639 314.
- 640 Lodolo, E., Tassone, A., Baradello, L., Lippai, H., Grossi, M., 2010. Morpho-bathymetric survey of Lago
641 Roca (Tierra del Fuego). *Bollettino di Geofisica Teorica ed Applicata*, 51, 125-125
- 642 Lodolo, E., Baradello, L., Darbo, A., Caffau, M., Tassone, A., Lippai, H., Lodolo, A., De Zorzi, G., Grossi,
643 M., 2012. Occurrence of shallow gas in the easternmost Lago Fagnano (Tierra del Fuego). *Near
644 Surface Geophysics*, 10, 161-169.
- 645 Lozano, J.G., Tassone, A., Lodolo, E., Menichetti, M., Cerredo, M.E., Bran, D., Esteban, F., Ormazabal,
646 J.P., Baradello, L., Vilas, J.F., 2018. Geophysical survey of Lago Yehuin: morphostructure and
647 sedimentary thickness, Fuegian Andes, Argentina. *Andean Geology*, in press.
- 648 Lyons, R.P., Scholz, C., Buoniconti, M.R., Martin, M.R., 2011. Late Quaternary stratigraphic analysis of
649 the Lake Malawi Rift, East Africa: An integration of drill-core and seismic-reflection data.
650 *Palaeogeography, Palaeoclimatology, Palaeoecology*, 303, 20-37.
- 651 Malumián, N., Olivero, E.B., 2006. El Grupo Cabo Domingo, Tierra del Fuego: bioestratigrafía,
652 paleoambientes y acontecimientos del Eoceno-Mioceno marino. *Revista de la Asociación
653 Geológica Argentina*, 61, 139-160.
- 654 Martinioni, D.R., Olivero, E.B., Medina, F.A., Palamarczuk, S., 2013. Cretaceous stratigraphy of Sierra
655 de Beauvoir, Fuegian Andes, Argentina. *Revista de la Asociación Geológica Argentina*, 70 (1),
656 70-95.
- 657 McCulloch, R.D., Fogwill, C.J., Sugden, D.E., Bentley, M.J., Kubi, P.W., 2005. Chronology of the last
658 glaciation in central Strait of Magellan and Bahía Inútil, southernmost South America.
659 *Geografiska Annaler: Series A, Physical Geography*, 87(2), 289-312.
- 660 Mendoza, L., Ritche, A., Fritsche, M., Hormaechea, J.L., Perdomo, R., Dietrich, R., 2015. Block
661 modeling of crustal deformation in Tierra del Fuego from GNSS velocities. *Tectonophysics*,
662 651-652, 58-65.
- 663 Mendoza, L., Perdomo, R., Hormaechea, J.L., Del Cogliano, D., Fritsche, M., Richter, A., Dietrich, R.,
664 2011. Present-day crustal deformation along the Magallanes-Fagnano Fault System in Tierra
665 del Fuego from repeated GPS observations. *Geophysical Journal International*, 184, 1009-
666 1022.
- 667 Meglioli, A., 1992. Glacial geology and chronology of southernmost Patagonia and Tierra del Fuego.
668 Argentina and Chile. Ph.D. thesis, Lehigh University.
- 669 Menichetti, M., Lodolo, E., Tassone, A., Geletti, R., 2001. Neotectonics at the continental Transform
670 boundary of the South America-Scotia plates: the Magallanes-Fagnano fault system. *Terra
671 Antarctic Publ 'Antarctic Neotectonic' workshop* 55, Siena.

- 672 Menichetti, M., Lodolo, E., Tassone, A., Hormaechea, J.L., Lippai, H., 2007a. Geologia dell'area del
673 Lago Fagnano in Terra del Fuoco (Sud America). *Rendiconti Online Società Geologica Italiana*,
674 4, 251-254.
- 675 Menichetti, M., Tassone, A., Flores, J., 2007b. Neotectonics and seismotectonics of the Tierra del
676 Fuego region. *Geosur 2007, Abstracts 127*, 100.
- 677 Menichetti, M., Lodolo, E., Tassone, A., 2008. Structural geology of the Fuegian Andes and Magallanes
678 fold-and-thrust belt – Tierra del Fuego Island. *Geologica Acta*, 6 (1), 19-42.
- 679 Mukasa, S.B., Dalziel, I.W.D., 1996. Southernmost Andes and South Georgia Island, North Scotia Ridge:
680 Zircon U-Pb and muscovite $^{40}\text{Ar}^{39}\text{Ar}$ age constraints on tectonic evolution of Southwestern
681 Gondwanaland. *Journal of South American Earth Sciences*, 9 (5-6), 349-365.
- 682 Nelson, E.P., Dalziel, I.W.D., Milnes, A.G., 1980. Structural geology of the Cordillera Darwin - collisional
683 style orogenesis in the southernmost Chilean Andes. *Eclogae Geologicae Helvetiae*, 73 (3),
684 727-751.
- 685 Olivero, E.B., Martinioni, D.R., 2001. A review of the geology of the Fuegian Andes. *Journal of South
686 American Earth Sciences*, 14, 175-188.
- 687 Olivero, E.B., Malumián, N., 2008. Mesozoic–Cenozoic stratigraphy of the Fuegian Andes, Argentina.
688 *Geologica Acta*, 6 (1), 5-18.
- 689 Pinson, L.J.W., Vardy, M.E., Dix, J.K., Henstock, T.J., Bull, J.M. Maclachlan, S.E., 2013. Deglacial history
690 of glacial lake Windermere, UK: implications for the Central British and Irish Sheet. *Journal of
691 Quaternary Sciences*, 28, 83-94.
- 692 Pugin, A., Pullan, S.E., Sharpe, D.R., 1999. Seismic facies and regional architecture of the Oak Ridges
693 Moraine area, southern Ontario. *Canadian Journal of Earth Sciences*, 36, 409-432
- 694 Rabassa, J., Coronato, A., Martinez, O., 2011. Late Cenozoic glaciations in Patagonia and Tierra del
695 Fuego: an updated review. *Biological Journal of the Linnean Society*, 103 (2), 316-335.
- 696 Sabbione, N., Connon, G., Buffoni, C., Hormaechea, J., 2016. Catálogo sísmico de referencia de Tierra
697 del Fuego. *Tierra del Fuego Reference Earthquake Catalogue*. Estación Astronómica Río
698 Grande.
- 699 Sabbione, N., Connon, G., Hormaechea, J., Rosa, M., 2007. Estudio de sismicidad en la provincia de
700 Tierra del Fuego, Argentina. *Geoacta*, 32, 41-50.
- 701 Scholz, C.A., 2001. Applications of seismic sequence stratigraphy in lacustrine basins. In: Last, W.M.,
702 Smol, J.P. (Eds.), *Tracking Environmental Change Using Lake Sediments. Developments in
703 Paleoenvironmental Research*. Springer, Dordrecht, 1, 7-22.
- 704 Scholz, C.A., Moore, Jr. T.C., Hutchinson, D.R., Golmshtok, A.Ja., Klitgord, K.D., Kuotchkin, A.G., 1998.
705 Comparative sequence stratigraphy of low-latitude versus high-latitude lacustrine rift basins:
706 seismic data examples from the East African and Baikal rifts. *Palaeogeography,
707 Palaeoclimatology, Palaeoecology*, 140, 401-420.
- 708 Suárez, M., Pettigrew, T.H., 1976. An upper Mesozoic island-arc–back-arc system in the southern
709 Andes and South Georgia. *Geological Magazine*, 113 (4), 305-328.

- 710 Tassone, A., Lippai, H., Lodolo, E., Menichetti, M., Comba, A., Hormaechea, J.L., Vilas, J.F., 2005. A
711 geological and geophysical crustal section across the Magallanes-Fagnano fault system in
712 Tierra del Fuego. *Journal of South American Earth Sciences*, 19, 99-109.
- 713 Tassone, A., Santomauro, M., Menichetti, M., Cerredo, M.E., Remesal, M.B., Lippai, H., Lodolo, E.,
714 Vilas, J.F., 2010. Imaging subsurface lithological and structural features by resistivity
715 tomography: North Beagle Channel (Tierra del Fuego, Argentina). *Revista Mexicana de*
716 *Ciencias Geológicas*, 27 (3), 562-572.
- 717 Tassone, A., Santomauro, M.G., Menichetti, M., Cerredo, M.E., Lodolo, E., Remesal, M.B., Lippai, H.,
718 Hormaechea, J.L., Vilas, J.F., 2011. ERT imaging of a shallow basin: Eastern Lago Fagnano,
719 Tierra del Fuego, Argentina. *Bollettino di Geofisica Teorica ed Applicata*, 52 (1), 9-21.
- 720 Torres Carbonell, P. J., Dimieri, L.V., Olivero, E.B., Bohoyo, F., Galindo-Zaldivar, J., 2014. Structure and
721 tectonic evolution of the Fuegian Andes (southernmost South America) in the framework of
722 the Scotia Arc development. *Global and Planetary Change*, 123 (B), 174-188.
- 723 Torres Carbonell, P. J., Dimieri, L.V., Martinioni, D.R., 2013. Early foreland deformation of the Fuegian
724 Andes (Argentina): constraints from the strain analysis of Upper Cretaceous-Danian
725 sedimentary rocks. *Journal of Structural Geology*, 48, 14-32.
- 726 Torres Carbonell, P.J., Dimieri, L.V., Olivero, E.B., 2011. Progressive deformation of a Coulomb thrust
727 wedge: the eastern Fuegian Andes thrust-fold belt. In: Poblet, J., Lisle, R. (Eds.), *Kinematic*
728 *evolution and structural styles of fold-and-thrust belts*. Geological Society, London, Special
729 *Publications*, 349, The Geological Society, Bath, 123-147.
- 730 Vail, P.R., Mitchum Jr, R.M., Thompson III, S., 1977. Seismic stratigraphy and global changes of sea
731 level: Part 3. Relative changes of sea level from Coastal Onlap: section 2. Application of
732 seismic reflection Configuration to Stratigraphic Interpretation.
- 733 Vail, P.R., 1987. Seismic Stratigraphy Interpretation using Sequence Stratigraphy, In *American*
734 *Association of Petroleum Geologists Studies in Geology*, 27 (1), 1-10.
- 735 van Wagoner, J.C., Mitchum, R.M., Posamentier, Jr. H.W., Vail, P.R., 1987. Key definitions of sequence
736 stratigraphy. In: Bally, A.W. (Ed.), *American Association of Petroleum Geologists Studies in*
737 *Geology*, 27 (1), 11-14.
- 738 Waldmann, N., Ariztegui, D., Anselmetti, F.S., Austin, J.A.Jr., Dunbar, R.B., Moy, C.M., Recasens, C.,
739 2008. Seismic stratigraphy of Lago Fagnano sediments (Tierra del Fuego, Argentina) - a
740 potential archive of Paleoclimatic change and tectonic activity since the Late Glacial.
741 *Geologica Acta*, 6, 101-110.
- 742 Waldmann, N., Ariztegui, D., Anselmetti, F.S., Austin, J.A.Jr, Moy, C.M., Stern, C., Recasens, C., Dunbar,
743 R.B., 2009. Holocene climatic fluctuations and positioning of the Southern Hemisphere
744 westerlies in Tierra del Fuego (54°S), Patagonia. *Journal Quaternary Sciences*, 25 (7), 1063-
745 1073.
- 746 Waldmann, N., Ariztegui, D., Anselmetti, F.S., Coronato, A., Austin, J.A.Jr., 2010a. Geophysical
747 evidence of multiple glacier advances in Lago Fagnano (54°S), southernmost Patagonia.
748 *Quaternary Science Review*, 29, 1188-1200.

- 749 Waldmann, N., Anselmetti, F.S., Ariztegui, D., Austin, J.A.Jr, Pirouz, M., Moy, C.M., Dunbar, R., 2010b.
750 Holocene mass-wasting events in Lago Fagnano, Tierra del Fuego (54° S): implications for
751 paleoseismicity of the Magallanes-Fagnano transform fault. *Basin Research*, 23 (2), 171-190.
- 752 Waldmann, N., Anselmetti, F.S., Ariztegui, D., Austin, Jr.J.A., Pirouz, M., Moy, C.M., Dunbar, R., 2011.
753 Holocene mass-wasting events in Lago Fagnano, Tierra del Fuego (54° S): implications for
754 paleoseismicity of the Magallanes-Fagnano transform fault. *Basin Research*, 23, 171-190.
- 755 Wessel, P., Smith, W.H.F., 1991. Free software helps map and display data. *EOS Transactions*
756 *American Geophysical Union*, 72 (41), 441-446.
- 757 Wilson, T.J., 1991. Transition from back-arc to foreland basin development in the southernmost
758 Andes: Stratigraphic record from the Ultima Esperanza District, Chile. *Geological Society of*
759 *America Bulletin*, 103 (1), 98-111.
- 760 Zanolla, C., Lodolo, E., Lippai, H., Tassone, A., Menichetti, M., Baradello, L., Grossi, M., Hormaechea,
761 J.L., 2011. Bathimetric map of Lago Fagnano (Tierra del Fuego Island). *Bollettino di Geofisica*
762 *Teorica ed Applicata*, 52, 1-8.

- We present a study of a seismic survey in Lago Chepelmut basin, located in Tierra del Fuego.
- Two seismic units are recognized within the basin, a glacial-related lower unit and a lacustrine upper unit.
- The basin is interpreted mainly as an ice-carved basin by the glacier lobes.
- We suggest that three major drops in the lake levels are evidenced in the stratigraphic record.